Dynamics exploration and aggressive maneuvering of a Longitudinal Vectored Thrust VTOL aircraft

Enrico Russo   Giuseppe Notarstefano   John Hauser

Abstract— In this paper we introduce the model of a Longitudinal Vectored Thrust Vertical Take Off and Landing (LVT-VTOL) aircraft. We believe that the proposed model, while described by reasonably tractable equations, captures several interesting dynamic features of new generation vectored thrust aerial vehicles with new maneuvering capabilities as, in particular, the ability of vertical take off and landing and transition to a (classical) forward flight configuration. We characterize the equilibrium manifold of the LVT-VTOL in the entire range of operation (from hover to forward flight). Then, as main contribution of the paper, we propose an optimal control based strategy to explore the trajectory manifold (the set of possibly aggressive trajectories) of the proposed model. To show the effectiveness of the exploration strategy, we compute a full transition from hover to forward flight.

I. INTRODUCTION

An interesting frontier in the design of aerial vehicles is the development of novel aircraft configurations that allow for a richer set of maneuvering capabilities. Inspired from standard architectures, designers are trying to develop new configurations that include in a unique vehicle the capabilities of rotor vehicles (mainly vertical take off and landing), fixed wing vehicles (agility in forward flight and energy efficiency) and thrusted vectored aircrafts (aggressive maneuvering).

The twin tilt-rotor V22-Osprey is certainly one of the most famous fixed wing aircrafts with vertical take off and landing capabilities. Recently, novel architectures have been proposed with a unique tilting rotor suitably placed in the fixed wing structure, see, e.g., patents [1], [2] and [3]. The control literature on tilt-rotor aircrafts is almost absent. In [4] and [5] a neural network and a backstepping based control law were proposed for a twin tilt-rotor architecture. In [6] the design, modeling, control and flight testing of a novel tilting wing quadrotor was presented. In [7] a nine degrees of freedom tilt-rotor aircraft model, inspired to the prototype proposed in patent [2], was introduced and analyzed when operating from near hover to forward flight maneuvers.

A wider literature can be found on vertical take off and landing aircrafts with capabilities of transition to forward flight. The well known flying wing Caltech Ducted Fan, developed at Caltech, was introduced in [8] and control strategies for transition maneuvers from hover to forward flight were studied in later works, see, e.g., [9]. More recently a novel architecture of a ducted fan UAV (Uninhabited Aerial Vehicle) was introduced in [10]. In [11] optimal transition

Enrico Russo and Giuseppe Notarstefano are with the Department of Engineering, University of Lecce, Via per Monteroni, 73100, Lecce, Italy (e-mail: {enricorusso82@gmail.it, giuseppe.notarstefano}@unile.it)

John Hauser is with the Department of Electrical and Computer Engineering, University of Colorado, Boulder, USA (e-mail: hauser@colorado.edu)
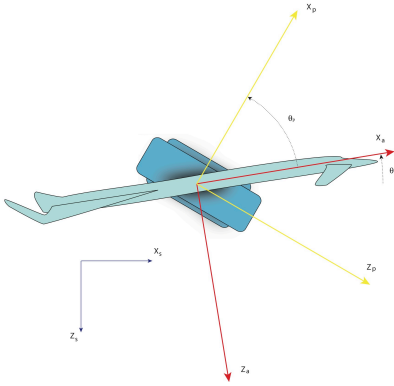
maneuvers for the UAV are computed by using a suitable optimization strategy.

In this paper we want to propose a simple longitudinal aircraft model that captures the main interesting features of aerial vehicle having: (i) an orientable thrust, (ii) vertical take off and landing capabilities, and (iii) capability of transitioning to a forward flight configuration. With such a model in hand we want to explore different dynamic and aerodynamic regimes. In particular, we aim at understanding how to design trajectories that involve a complete transition from hover to forward flight. The main contribution of the paper is threefold. First, we introduce a planar model of a Longitudinal Vectored Thrust VTOL aircraft suitable for optimization and control. We call this model LVT-VTOL. Second, we characterize the equilibrium manifold of the LVT-VTOL aircraft. That is, we study stationary (trimming) trajectories of the vehicle over the entire operating region. In particular, we focus on the two extreme regions, namely hover and forward flight and show what happens in the overlapping region. Third, we explore the dynamic capabilities of the vehicle by use of optimal control tools. We provide a strategy to compute non-stationary trajectories of the LVT-VTOL, based on the Projection Operator Newton method for optimization of trajectory functionals, [12]. To show the effectiveness of this tool we compute a complete transition maneuver from hovering to forward flight.

II. THE LVT-VTOL AIRCRAFT MODEL

The LVT-VTOL aircraft model, whose scheme is depicted in Figure 1, consists of two rigid bodies, a propulsion unit and a fixed wing body, linked together through a joint that allows the propulsive unit to direct the thrust in any direction. Thanks to the orientable thrust the aircraft can operate in a hovering regime (so that it can take off and land vertically) and standard forward flight regime together with any combination of the two.

The controls acting on the LVT-VTOL are the thrust force, the torque to orient the propulsion unit, the elevator deflection on the fixed-wing body and the deflection of a movable vane located at the bottom of the propulsion unit.

Next, we introduce three reference frames that will be useful in the development of the LVT-VTOL dynamic model. Formally, we have the following reference frames and parameters of the rigid bodies

- F^s - **Spatial** Frame. It is a fixed inertial frame with x-z axes oriented in a north-down fashion.
- F^a - **Aircraft** Frame. It is a frame attached to the fixed wing *'aircraft'* body. The center of mass of the rigid

Fig. 1: LVT-VTOL aircraft model with reference frames

body is located at (x_c, z_c) in this reference frame and the body mass is m_a. The moment of inertia about the center of mass of the rigid body is I_y^a.

- F^p - **Propulsion** Frame. It is a frame attached to the propulsion unit. In this frame the center of mass of the rigid body is located at $(0,0)$ with mass m_p. The moment of inertia about the center of mass is I_y^p.

We take the point of intersection of the joint hinging the rigid bodies as the origin for the aircraft and propulsion frames.

We compute the aircraft dynamic model by use of the *Lagrangian analysis*. The set of *generalized coordinates* that describes our model is

$$q = (x, z, \theta, \theta_p)$$

where the subscript p for θ_p stands for "propulsion unit". Referring to Figure 1, (x, z) is the spatial position of the fixed wing body (and thus of the aircraft) with respect to the inertial (spatial) frame; the angles θ and θ_p parameterize the orientation of the aircraft frame F^a with respect to the inertial frame and the propulsion frame F^p with respect to the aircraft frame respectively.

The propulsion pitch angle θ_p is defined so that in *hover* $\theta_p \approx \frac{\pi}{2}$, while $\theta_p \approx 0$ in forward flight. To be consistent with real aircrafts, we restrict the range of operation of our aircraft model so that the value of θ is bounded by $\|\theta\| < \frac{\pi}{2}$ and the value of θ_p is restricted to $-\frac{\pi}{4}$ and $\frac{3\pi}{4}$.

Let $\boldsymbol{q} = \begin{bmatrix} x & z & \theta & \theta_p \end{bmatrix}^T$, the LVT-VTOL *planar* dynamic model is given by the system of dynamic equations $\boldsymbol{M}(\boldsymbol{q})\ddot{\boldsymbol{q}} + \boldsymbol{C}(\boldsymbol{q}, \dot{\boldsymbol{q}}) + \boldsymbol{G}(\boldsymbol{q}) = \boldsymbol{\Upsilon}$, where the mass matrix $\boldsymbol{M}(\boldsymbol{q})$, the *Coriolis* vector $\boldsymbol{C}(\boldsymbol{q}, \dot{\boldsymbol{q}})$ and the *gravity* vector $\boldsymbol{G}(\boldsymbol{q})$ are exploited in (1), while the vector of generalized forces and moments $\boldsymbol{\Upsilon}$ will be specified in the next section. For the sake of compactness we sometimes use the notations c_θ and s_θ for $\cos\theta$ and $\sin\theta$ respectively.

III. AERODYNAMICS AND CONTROLS

In this section we exploit the external forces and moments generated by the propulsion unit and by the aerodynamics.

A. Aerodynamics of the fixed wing body

We use a standard formulation in flight dynamics for the aerodynamic forces and moments, [13], [14]. The longitudinal aerodynamic force is the sum of two perpendicular

components: the *Drag* (directed along the airflow velocity) and the *Lift* (perpendicular to the airflow direction). A pitching moment is also taken into account when the pitch-axis does not pass through the *center of pressure*. Formally, let F_w denote the classical wind frame, i.e., a reference frame whose x-axis points in the direction of the velocity vector, and the z axis is chosen so that vectors in the wind frame are transformed into the body frame with a simple rotation

$$\boldsymbol{R}_{-\alpha} = \begin{bmatrix} \cos\alpha & -\sin\alpha \\ \sin\alpha & \cos\alpha \end{bmatrix}.$$

The angle α is called *angle of attack* and is defined as $\tan\alpha = \frac{v_{az}}{v_{ax}}$, where $\boldsymbol{v}_a = (v_{ax}, v_{az})^T$ is the velocity of the aerodynamic center expressed in the body frame F_a.

Aerodynamic forces (Drag and Lift) are conventionally expressed in *wind-frame* coordinates in terms of dimensionless coefficients called aerodynamic coefficients, i.e.

$$\begin{bmatrix} D \\ L \end{bmatrix} = \frac{1}{2}\rho\|\boldsymbol{v}_a\|^2 S \begin{bmatrix} C^D(\alpha) + C^D_{\delta_e}(\alpha)\delta_e \\ C^L(\alpha) + C^L_{\delta_e}(\alpha)\delta_e \end{bmatrix}$$

where ρ is the air density, S is the wetted surface of the fixed wing body, $\boldsymbol{v}_a$ is the velocity of the fixed wing body aerodynamic center and δ_e is the elevator deflection.

Figure 2 shows a scheme of the drag and lift forces together with the wind, body and inertial reference frames.
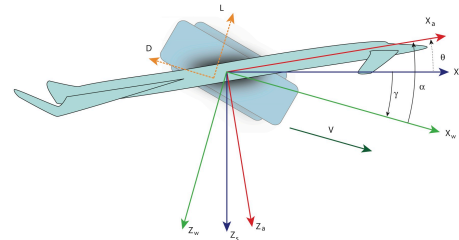

Fig. 2: Lift and Drag of the fixed wing body and reference frames

Sometimes it is more convenient to express the aerodynamic forces in the body-frame in terms of equivalent aerodynamic coefficients. Let $C^X(\alpha)$ and $C^Z(\alpha)$ be the aerodynamic coefficients in the body-frame with $C^X_{\delta_e}(\alpha)$ and $C^Z_{\delta_e}(\alpha)$ the derivatives with respect to the elevator deflection. The aerodynamic forces in body-frame coordinates are

$$\boldsymbol{F}_a^a = \begin{bmatrix} F_{a_x}^a \\ F_{a_z}^a \end{bmatrix} = \frac{1}{2}\rho\|\boldsymbol{v}_a\|^2 S \begin{bmatrix} C^X(\alpha) + C^X_{\delta_e}(\alpha)\delta_e \\ C^Z(\alpha) + C^Z_{\delta_e}(\alpha)\delta_e \end{bmatrix}. \quad (2)$$

The aerodynamic (pitching) moment is expressed directly in the body frame and is given by

$$M_a = \frac{1}{2}\rho V^2 S \bar{c} C_m \quad (3)$$

where $\bar{c}$ is the length of the *chord* of the wing.

Since we are interested in designing maneuvers in the entire range of operation of the LVT-VTOL, i.e. from vertical take off to forward flight, we need an expression for the aerodynamic coefficients over the entire range of angles of attack (thus also where they are not conventionally defined).

We propose an analytic expression for the drag, lift and moment coefficients over the range of the angles of attack

$$\begin{bmatrix} m_a + m_p & 0 & m_a(z_c c_\theta - x_c s_\theta) & 0 \\ 0 & m_a + m_p & -m_a(z_c s_\theta + x_c c_\theta) & 0 \\ m_a(z_c c_\theta - x_c s_\theta) & -m_a(z_c s_\theta + x_c c_\theta) & m_a(x_c^2 + z_c^2) + I_y^a + I_y^p & I_y^p \\ 0 & 0 & I_y^p & I_y^p \end{bmatrix} \begin{bmatrix} \ddot{x} \\ \ddot{z} \\ \ddot{\theta} \\ \ddot{\theta}_p \end{bmatrix} + \begin{bmatrix} -m_a\dot\theta^2(z_c s_\theta + x_c c_\theta) \\ -m_a\dot\theta^2(z_c c_\theta - x_c s_\theta) \\ 0 \\ 0 \end{bmatrix} + \begin{bmatrix} 0 \\ -(m_a + m_p)g \\ m_a g(z_c s_\theta + x_c c_\theta) \\ 0 \end{bmatrix} = \boldsymbol{\Upsilon}$$

(1)

$[-\pi, \pi]$. We use sinusoidal functions that preserve the main coefficients shape in standard regimes. For example, the drag coefficient is positive in the entire range and in forward flight is an even function of the angle of attack. The lift and moment coefficients range from negative to positive values and in forward flight are odd functions of the angle of attack with respectively positive and negative derivatives. A similar model was proposed in [15]. The analytic expressions are

$$C^D = A^D \cos(\omega^D \alpha + \phi^D) + h_D$$
$$C^L = A^L \sin(\omega^L \alpha + \phi^L) + h_L$$
$$C^M = A^M \sin(\omega^M \alpha + \phi^M) + h_M$$
$$C_{\delta_e}^D = A_{\delta_e}^D \sin(\omega_{\delta_e}^D \alpha) + \phi^D) + h_{\delta_e}^D$$
$$C_{\delta_e}^L = A_{\delta_e}^L \sin(\omega_{\delta_e}^L \alpha + \phi_{\delta_e}^L) + h_{\delta_e}^L$$
$$C_{\delta_e}^M = A_{\delta_e}^M \cos(\omega_{\delta_e}^M \alpha + \phi_{\delta_e}^M) + h_{\delta_e}^M,$$

where the sinusoids coefficients used in the paper are

$A^D = 1$	$\omega^D = 2$	$\phi^D = 0$	$h^D = $ -2
$A_{\delta_e}^D = 1.87 \cdot 10^{-4}$	$\omega_{\delta_e}^D = 2.58$	$\phi_{\delta_e}^D = $ -0.87	$h_{\delta_e}^D = 10^{-4}$
$A^L = $ -6.5 $\cdot$ 1.7	$\omega^L = 2$	$\phi^L = 0$	$h^L = 2$
$A_{\delta_e}^L = 3.9 \cdot 10^{-2}$	$\omega_{\delta_e}^L = 0.55$	$\phi_{\delta_e}^L = $ -0.61	$h_{\delta_e}^L = $ -3.2
$A^M = $ -0.2	$\omega^M = 1$	$\phi^M = 0$	$h^M = 0$
$A_{\delta_e}^M = 0.0013$	$\omega_{\delta_e}^M = 3.1$	$\phi_{\delta_e}^M = $ -0.018	$h_{\delta_e}^M = 9 \cdot 10^{-3}$

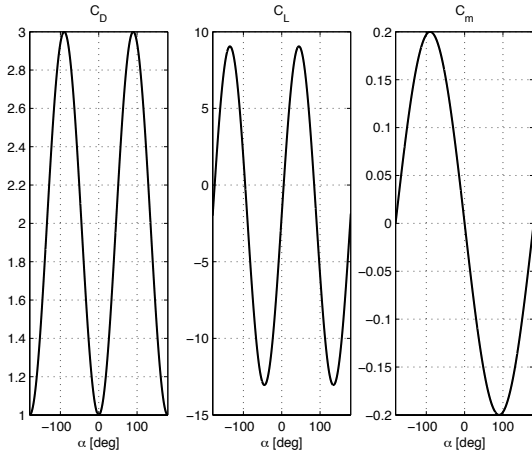while the behavior of C^D, C^L and C^M with respect to α is depicted in Figure 3.

Fig. 3: Aerodynamic coefficients C^D, C^L and C^M for $\alpha \in [-\pi, \pi]$

Let $\boldsymbol{x}_a = \begin{bmatrix} x_a & z_a \end{bmatrix}^T$ be the position of the aerodynamic center of the wing in the aircraft frame. Then its position in the inertial frame is given by $\boldsymbol{x}_a^s = \boldsymbol{x} + \boldsymbol{R}_\theta \boldsymbol{x}_a$, where $\boldsymbol{x}$ is the position of F^a with respect to the inertial frame F^s and

$$\boldsymbol{R}_\theta = \begin{bmatrix} \cos\theta & \sin\theta \\ -\sin\theta & \cos\theta \end{bmatrix}.$$

The linear velocity of the aerodynamic center is given by:

$$\dot{\boldsymbol{x}}_a^s = \dot{\boldsymbol{x}} + \dot{\boldsymbol{R}}_a \boldsymbol{x}_a = \begin{bmatrix} \dot{x} - \dot{\theta}(x_a s\theta - z_a c\theta) \\ \dot{z} - \dot{\theta}(x_a c\theta + z_a s\theta) \end{bmatrix} = \boldsymbol{J}_a(\boldsymbol{q})\dot{\boldsymbol{q}}$$

where

$$\boldsymbol{J}_a(\boldsymbol{q}) = \begin{bmatrix} 1 & 0 & z_a c\theta - x_a s\theta & 0 \\ 0 & 1 & -x_a c\theta - z_a s\theta & 0 \end{bmatrix}$$

is the Jacobian expressing $\dot{\boldsymbol{x}}_a^s$ in generalized coordinates.

The aerodynamic force expressed in the inertial frame is obtained from the force in the body frame by a rotation of θ, that is $\boldsymbol{F}_a^s = \boldsymbol{R}_\theta \boldsymbol{F}_a^a$, so that the vector $\boldsymbol{\tau}_{a,a}$ of *generalized forces and moments* due to $\boldsymbol{F}_a^s$ is given by

$$\boldsymbol{\tau}_a = \begin{bmatrix} F_{a_x}(\delta_e) \\ F_{a_z}(\delta_e) \\ M_{F_a}(\delta_e) \\ 0 \end{bmatrix} = \boldsymbol{J}_a^T(\boldsymbol{q}) \boldsymbol{F}_a^s.$$

The aerodynamic moment M_a in (3) is also the generalized moment along the velocity $\dot\theta$ (while no other contributions are generated by M_a along the other generalized velocities).

B. Aerodynamics of the movable vanes

The *movable vanes* are little wings located at the bottom of the propulsion unit. We consider two movable vanes and model both of them as a single wing capable of generating a threefold aerodynamic action (drag and lift forces and a pitching moment) as depicted in Figure 4. The force vector generated by the movable vanes is given by

$$\boldsymbol{F}_v^w = \begin{bmatrix} D_v \\ L_v \end{bmatrix} = -\rho V_{vane}^2 S_v \delta_v \begin{bmatrix} C_v^D \\ C_v^L \end{bmatrix}, \qquad (4)$$

where S_v is the surface of the movable vane and V_{vane} is the airspeed in the propulsion unit wash. The force is expressed in the "vanes wind-frame" , which is coincident with the propulsion frame F^p, since the air flow is oriented as the propulsion bucket. This force is applied at the pressure point $(-h_{vane}, r_{vane})$, measured in the propulsion frame. This provides an additional pitching moment M_{F_v}. The aerodynamic moment, expressed in the body (propulsion) frame, is given by

$$M_v = \rho V_{vane}^2 c_v S_v C_{m_v} \delta_v.$$

We assume that C_v^D, C_v^L and C_v^m are constant since we expect the angle δ_v to be reasonably small.

Using classical actuator theory, [16], it is possible to obtain an expression of the airspeed V_{vane} in terms of the thrust T. In the paper we set $V_{vane} = c_0 T^{\frac{1}{2}}$, where c_0 is a constant depending on the propulsion unit physical properties.
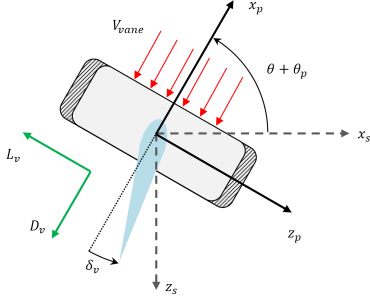
Fig. 4: Movable vanes taken as a single wing who provide a double aerodynamic action by the deflection δ_v through the airspeed V_{vane}

The aerodynamic force generated by the movable vanes expressed in the inertial frame is obtained by rotating the force in equation (4) of an angle $\theta + \theta_p$, i.e.

$$\boldsymbol{F}_v^s = -\rho V_{vane}^2 S_v \delta_v \begin{bmatrix} \cos(\theta + \theta_p) & \sin(\theta + \theta_p) \\ -\sin(\theta + \theta_p) & \cos(\theta + \theta_p) \end{bmatrix} \begin{bmatrix} C_v^D \\ C_v^L \end{bmatrix}.$$

The vector $\boldsymbol{\tau}_v$ of generalized forces and moments due to the force $\boldsymbol{F}_v^s$ is obtained by computing the Jacobian $\boldsymbol{J}_v$ along the same line as in the previous section, so that

$$\boldsymbol{\tau}_v = \begin{bmatrix} F_{v_x}(\delta_v, T) \\ F_{v_z}(\delta_v, T) \\ M_{F_v}(\delta_v, T) \\ M_{F_v}(\delta_v, T) \end{bmatrix} = \boldsymbol{J}_v^T(\boldsymbol{q}) \boldsymbol{F}_v^s.$$

C. Vector of generalized forces/moments and control inputs

We are now ready to provide an explicit expression for the vector of generalized forces and moments $\boldsymbol{\Upsilon}$ in (1).

The forces and moments acting on the LVT-VTOL are:

- the thrust force provided by the propulsion unit and acting on the center of mass of the propulsion unit body.
- the control torque τ_p to tilt the propulsion unit.
- the aerodynamic forces and moments acting on the *fixed wing body*.
- the aerodynamic forces and moments provided by the movable vanes at the bottom of the propulsion bucket.

Remark 3.1: In our model we neglect the aerodynamics generated by the surface of the propulsion unit as well as the derivatives of the aerodynamic input controls. □

Since the thrust force is applied at the center of mass of the propulsion unit (thus at the center of the *body* and *propulsion* frames), the generalized thrust forces, T_x and T_z, are

$$T_x = T \cos(\theta + \theta_p)$$
$$T_z = -T \sin(\theta + \theta_p),$$

The torque τ_p acts directly on the velocity $\dot{\theta}_p$ and thus affects only the generalized moment along the velocity $\dot{\theta}_p$.

Thus, component-wise the vector $\boldsymbol{\Upsilon}$ is given by:

$$\begin{aligned} \Upsilon_x &= F_{a_x}(\delta_e) + F_{v_x}(\delta_v, T) + T \cos(\theta + \theta_p) \\ \Upsilon_z &= F_{a_z}(\delta_e) + F_{v_z}(\delta_v, T) - T \sin(\theta + \theta_p) \\ \Upsilon_\theta &= M_a(\delta_e) + M_{F_a}(\delta_e) + M_{F_v}(\delta_v, T) \\ \Upsilon_{\theta_p} &= M_v(\delta_v) + M_{F_v}(\delta_v, T, \alpha, \alpha_p) + \tau_p \end{aligned}$$

where $\boldsymbol{F}_a$ and $\boldsymbol{F}_v$ are the aerodynamic forces acting on the fixed wing body and movable vanes respectively (i.e., at their aerodynamic centers), M_{F_a}, M_{F_v} are the pitching moments due to the aerodynamic forces (applied at the aerodynamic center, which in general is different from the center of mass), M_a, M_v are aerodynamic (pitching) moments with respect to the aerodynamic center, T is the magnitude of the thrust force directed along the positive x axis of the propulsion frame F_p (applied at the center of the reference frame), and τ_p is the control torque acting at the pitch joint.

The generalized forces and moments depend on the vector of control inputs

$$\boldsymbol{u} = \begin{bmatrix} T & \tau_p & \delta_e & \delta_v \end{bmatrix}^T.$$

IV. EQUILIBRIUM MANIFOLD

In this section we analyze the equilibrium manifold of the LVT-VTOL, i.e. the set of all flight trajectories for which the dynamically important variables are constant. The key purpose of this study is to develop an understanding of the range of model validity. In the flight dynamics literature these "constant trajectories" are often referred to as trimming trajectories and the procedure of computing them is known as "trimming the aircraft". For the LVT-VTOL aircraft, we require the propulsion unit angle θ_p to be constant. This implies that the system may be treated as a typical aircraft, with the exception that hovering is possible. Finding constant trajectories requires the solution of a set of nonlinear equations expressing the fact that all accelerations must be zero. Thus, a trimming trajectory is given by the configuration of generalized coordinates and control inputs such that

$$\boldsymbol{M}(\boldsymbol{q})^{-1}[-\boldsymbol{C}(\boldsymbol{q}, \dot{\boldsymbol{q}})\dot{\boldsymbol{q}} - \boldsymbol{G}(\boldsymbol{q}) + \boldsymbol{\Upsilon}] = 0, \qquad (5)$$

which can be written as: $g(\theta, \theta_p, \dot{x}, \dot{z}, T, \tau_p, \delta_e, \delta_v) = 0$, where $g : \mathbb{R}^8 \to \mathbb{R}^4$ is suitably defined. Thus, we need to solve a system of four nonlinear equations in eight unknowns. We parametrize the trimming trajectories by using the propulsion unit orientation θ_p, the velocity $V = \sqrt{\dot{x}^2 + \dot{z}^2}$ and the flight-path angle γ (i.e. the angle between the velocity vector and the inertial frame horizontal axis).

In the equilibrium manifold computation, we assume that the movable vanes are useful in hover and vertical flight, but irrelevant in forward flight, while the elevator is significant only in forward flight. Thus, we set $\delta_e = 0$ when computing the equilibrium manifold in hover and vertical take off, and, $\delta_v = 0$ in forward flight. We expect this condition to hold approximately also in neighboring regions.

To compute the equilibrium manifold in hover and vertical flight we gather the values for T (thrust), τ_p (pitch-joint torque), δ_v (movable vanes deflection) and θ (pitch angle) solving system (5) for different values of velocity and propulsion angle. That is, set the constant values for speed, flight-path angle (in this case $\gamma = \pi/2$) and propulsion angle, we compute the control inputs and the angle of attack that trim the dynamic model. Varying the given parameters we obtain the sequences of equilibria in Figure 5.

The same test is performed for the forward flight configuration, i.e. $\gamma = 0$. Looking at the behavior of the
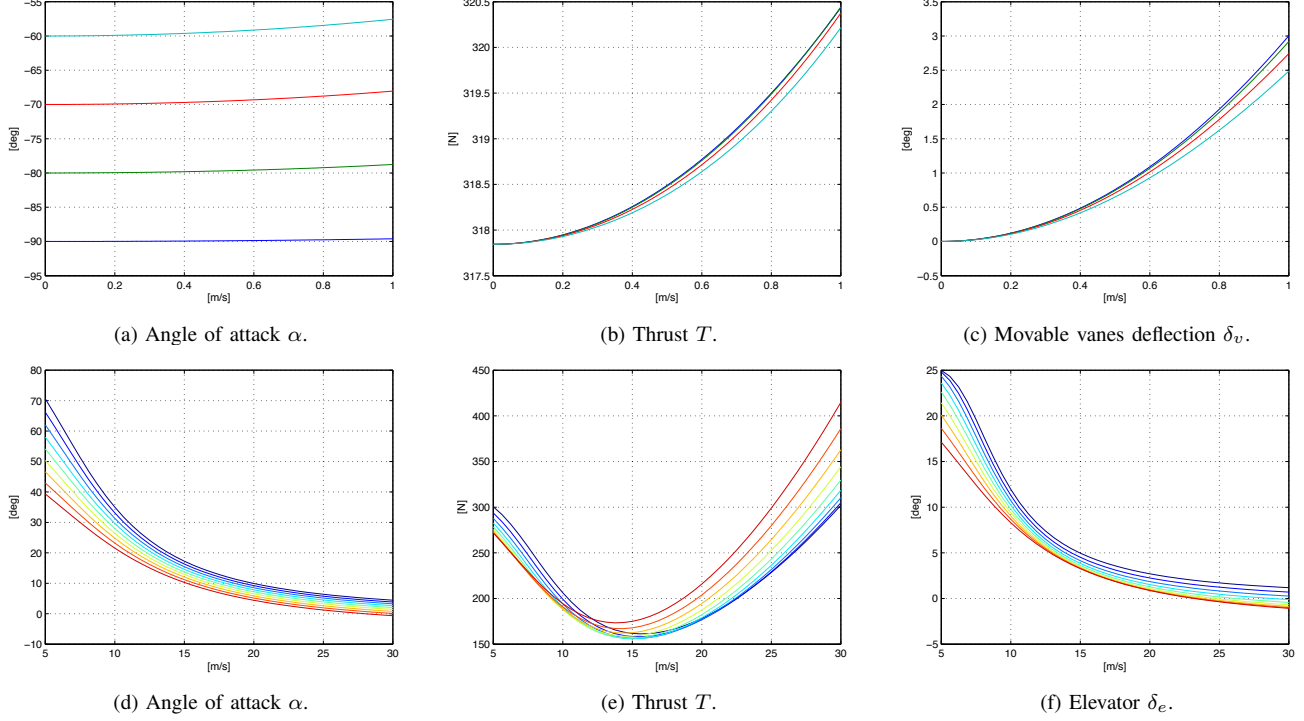
Fig. 5: Equilibrium manifold for: (i) hover to vertical flight (a-c) and constant altitude forward flight (d-f). Specifically: (i) $V = 0 \div 1$ m/s, γ=90 deg, θ_p=(90, 80, 70, 60) deg (blue to cyan), and (ii) $V = 5 \div 30$ m/s, γ=0 deg, $\theta_p = 0 \div 40$ deg.

dynamic model at slower speed, we see that the angle of attack increases toward the value $\pi/2$ (Figure 5d) if the propulsion angle is small (the LVT-VTOL needs a higher angle of attack in order to balance gravity by the thrust and to increase the lift force), whereas it tends to decrease when the propulsion is rotated. This provides useful hints for the transition maneuvers.

V. TRAJECTORY EXPLORATION VIA LEAST SQUARE OPTIMAL CONTROL

Complex dynamic interactions make the development of maneuvers highly nontrivial. To this end, we use nonlinear least squares trajectory optimization to explore system trajectories. That is, we consider the optimal control problem

$$\min \quad \|(x(\cdot), u(\cdot)) - (x_d(\cdot), u_d(\cdot))\|^2_{L_2}/2$$
$$\text{subj} \quad \dot{x} = f(x, u), \quad x(0) = x_0,$$

where $\| \cdot \|_{L_2}$ is a weighted L_2 norm on $[0, T]$ [1] and $(x_d(\cdot), u_d(\cdot))$ is a desired curve used as a trajectory exploration design *parameter*. Writing the least squares trajectory functional as $h(\xi) = \|(x(\cdot), u(\cdot)) - (x_d(\cdot), u_d(\cdot))\|^2_{L_2}/2$ with $\xi = (x(\cdot), u(\cdot))$, the optimization problem becomes

$$\min_{\xi \in \mathcal{T}} h(\xi) \tag{6}$$

where $\mathcal{T}$ is the manifold of bounded trajectories $(x(\cdot), u(\cdot))$ on $[0, T]$. To facilitate the local exploration of trajectories of

---

[1] The L_2 weights are design variables that reflect the relative importance (or confidence) of certain components of the desired curve.

this highly coupled nonlinear system, we use the Projection Operator Newton method developed in [12], see also [17]. The time varying trajectory tracking control law

$$\dot{x} = f(x, u), \qquad x(0) = x_0,$$
$$u(t) = \mu(t) + K(t)(\alpha(t) - x(t))$$

defines the projection operator $\mathcal{P} : \xi = (\alpha, \mu) \mapsto \eta = (x, u)$, taking the curve $\xi = (\alpha, \mu)$ to the trajectory $\eta = (x, u)$. Using the projection operator to locally parametrize the trajectory manifold, we may convert the constrained optimization problem (6) into one of minimizing the unconstrained functional $g(\xi) = h(P(\xi))$. Minimization of the trajectory functional is accomplished by iterating over the following Newton descent method, where ξ_i indicates the current trajectory iterate and ξ_0 is an initial trajectory.

Algorithm (projection operator Newton method)
Given initial trajectory $\xi_0 \in \mathcal{T}$
For $i = 0, 1, 2...$

    design K defining $\mathcal{P}$ about ξ_i
    search direction

$$\zeta_i = \arg \min_{\zeta \in T_{\xi_i}\mathcal{T}} Dg(\xi_i) \cdot \zeta + \frac{1}{2} D^2 g(\xi_i)(\zeta, \zeta)$$

    step size $\gamma_i = \arg \min_{\gamma \in (0,1]} g(\xi + \gamma \zeta_i)$;
    project $\xi_{i+1} = \mathcal{P}(\xi_i + \gamma_i \zeta_i)$.

end

Note that the two main steps of designing the K and searching for the descent direction involve the solution of suitable (well known) LQ optimal control problems.

(a) $\dot{x}$ (b) $\dot{z}$ (c) Pitch angle θ

(d) Propulsion orientation θ_p (e) Elevator δ_e (f) Movable vanes deflection δ_v
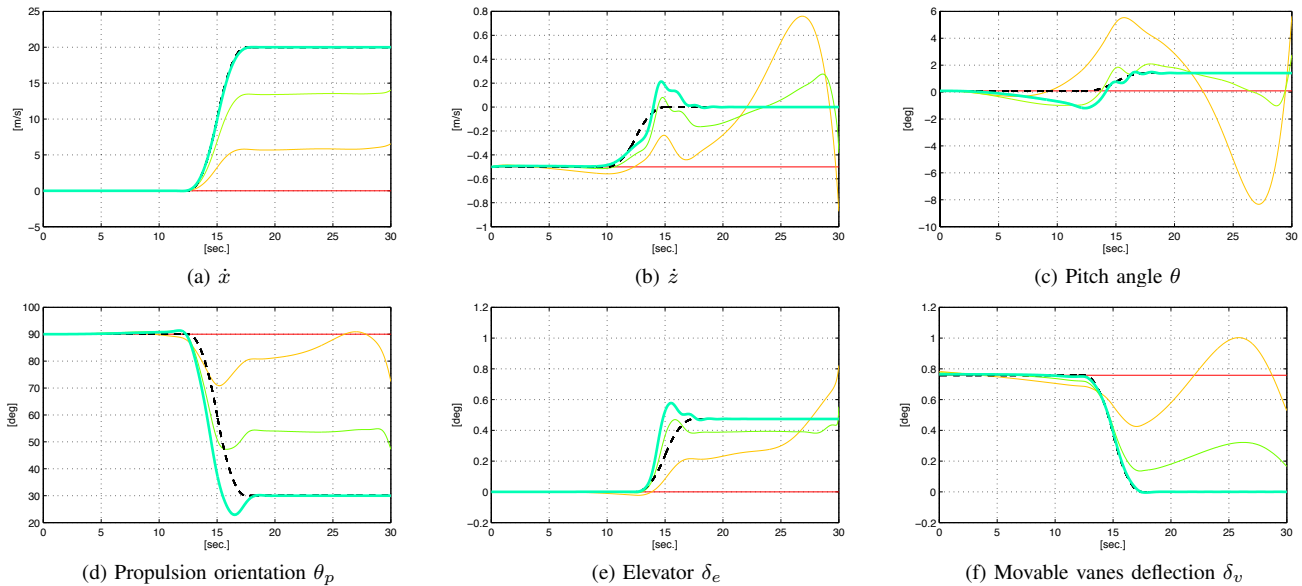
Fig. 6: Trajectory exploration: vertical take-off/forward flight transition for the LVT-VTOL. Specifically: vertical take-off at $V = 0.5 m/s$, $\theta_p = 90, \deg$; change of flight-path angle from 90 to 0 degree with forward speed $V = 0 \div 20 m/s$, $\theta_p = 30, \deg$. The desired curve is the thick dashed line, the optimal trajectory is the thick solid line, while the light solid lines are trajectories of the intermediate instances of the projection operator Newton method.

A. The vertical take-off/forward flight transition

We compute a transition maneuver from hovering ($\dot{z} = -0.5 m/s$ and $\theta_p = \pi/2$) to forward flight ($\dot{x} = 20 m/s$ and $\theta_p \simeq 0$). In the computation of this transition, a very naive choice was made for the desired trajectory. The two stationary conditions at hover and forward flight (with corresponding propulsion angles) were computed and then a smooth transition of all configuration variables was chosen. Nevertheless, the optimization procedure provides an interesting transition trajectory that satisfies the system dynamics. In effect, the optimization works to *spread out* the inconsistencies in the desired trajectory to obtain a dynamically feasible trajectory. The curves in Figure 6 depict the result of the optimization procedure with a choice of L_2 weights for measuring the distance between curves. For this choice, the velocities follow the desired curves in a reasonable manner. In contrast, the propulsion angle and the elevator exhibit interesting lead and overshoot phenomena that deserve further attention in the future. Some of the most interesting excursions from the *desired* (unrealistic) curves are those associated with the aircraft pitch attitude and elevator. As noted above, the desired curves were chosen as a smooth combination of two sets of equilibrium values without reflecting what is needed during maneuvering. To make up for this naive choice of the desired curve, the optimization has found that a temporary decrease (increase) in the pitch (elevator) helps in the execution of the maneuver.

REFERENCES

[1] R. N. Pham, "High performance VTOL convertiplanes," United States, Patent US6974105, December 2005.

[2] P. Mioduchevski, "Convertible aircraft," Europe, Assignee: International Aviation Supply I.A.S. S.R.L., Brindisi, IT), Patent EP1999016, 2008.

[3] R. G. Burrage, "Tilt-rotor aircraft," United States, Patent US7584923, September 2009.

[4] A. Calise and R. T. Rysdyk, "Nonlinear adaptive flight control using neural networks," *IEEE Control Systems Magazine*, vol. 18, no. 6, pp. 14–25, Dec. 1998.

[5] F. Kendoul, I. Fantoni, and R. Lozano, "Modeling and control of a small autonomous aircraft having two tilting rotors," *IEEE Trans Robotics*, vol. 22, no. 6, pp. 1297–1302, Dec. 2006.

[6] K. Nonami, F. Kendoul, S. Suzuki, W. Wang, and D. Nakazawa, *Autonomous Flying Robots: Unmanned Aerial Vehicles and Micro Aerial Vehicles*, 1st ed. Springer, 2010.

[7] G. Notarstefano and J. Hauser, "Modeling and dynamic exploration of a Tilt-Rotor VTOL aircraft," in *Proc NOLCOS*, Bologna, Italy, September 2010.

[8] A. Jadbabaie, J. Yu, and J. Hauser, "Receding horizon control of the caltech ducted fan: a control lyapunov function approach," in *IEEE Int. Conf. on Control Applications*, vol. 1, Kohala Coast, HI, USA, 1999, pp. 51–56.

[9] A. Jadbabaie and J. Hauser, "Control of a thrust-vectored flying wing: a receding horizon - lpv approach," *International Journal of Robust and Nonlinear Control*, vol. 12, no. 9, pp. 869–896, 2002.

[10] L. Marconi and R. Naldi, "Nonlinear robust control of a reduced-complexity ducted mav for trajectory tracking," in *Proc CDC*, San Diego, CA, December 2006.

[11] R. Naldi and L. Marconi, "Optimal transition maneuvers for a class of V/STOL aircraft," *Automatica*, vol. 47, 2011.

[12] J. Hauser, "A projection operator approach to the optimization of trajectory functionals," in *IFAC World Congress*, Barcelona, 2002.

[13] B. Ektin and L. D. Reid, *Dynamics of Flight*, J. Wiley and I. Sons, Eds. John Wiley and Sons, Inc, 1965.

[14] B. L. Stevens and F. L. Lewis, *Aircraft Control and Simulation*, J. Wiley and I. Sons, Eds. John Wiley and Sons, Inc, 2003.

[15] M. Milam, R. M. Murray, R. Franz, and J. E. Hauser, "Receding horizon control of a vectored thrust flight experiment," *IEE Proc. Control Theory and Applications*, April 2003.

[16] R. Stengel, *Flight Dynamics*. Princeton University Press, 2004.

[17] J. Hauser and D. G. Meyer, "The trajectory manifold of a nonlinear control system," in *Proc CDC*, vol. 1, December 1998, pp. 1034–1039.